JOURNAL OF GEOPHYSICAL RESEARCH, VOL. 100, NO. D4, PAGES 7381–7396, APRIL 20, 1995

Modeled impacts of stratospheric ozone and water vapor perturbations with implications for high-speed civil transport aircraft

David Rind and Patrick Lonergan[1]
NASA Goddard Space Flight Center, Institute for Space Studies, New York

Abstract. Ozone and water vapor perturbations are explored in a series of experiments with the Goddard Institute for Space Studies climate/middle atmosphere model. Large perturbations to stratospheric ozone and water vapor are investigated, with and without allowing sea surface temperatures to change, to illuminate the nature of the dynamic and climatic impact. Then more realistic ozone and water vapor perturbations, similar to those estimated to result from aircraft emissions, are input and the equilibrium response obtained. Removing ozone in the lower stratosphere without allowing sea surface temperatures to change results in in situ cooling of up to 10°C in the tropical lower stratosphere, with radiative warming about half as large in the middle stratosphere. The temperature changes induce increases in tropospheric and lower stratospheric eddy energy and in the lower stratosphere residual circulation of the order of 10%. When sea surface temperatures are allowed to respond to this forcing, the global, annual-average surface air temperature cools by about 1°C as a result of the decreased ozone greenhouse capacity, reduced tropospheric water vapor, and increased cloud cover. For more realistic ozone changes, as defined in the High-Speed Research Program/Atmospheric Effects of Stratospheric Aircraft reports, the stratosphere generally cools by a few tenths degrees Celsius. In this case, the surface air temperature change is not significant, due to the conflicting influences of stratospheric ozone reduction and tropospheric ozone increase, although high-latitude cooling of close to 0.5°C does occur consistently. Doubled stratospheric water vapor cools the middle atmosphere by 2°–3°C and warms the upper troposphere by 0.5°C. Reduced tropospheric-stratospheric vertical stability leads to tropospheric planetary longwave energy increases of some 15% for the longest waves and stratospheric residual circulation increases of 5%. When sea surface temperatures are allowed to change, the surface air temperature warms by just a few tenths of a degree Celsius; although this change is not significant in terms of the model's natural variability, the experiment is warmer than the control in most years. The response is muted as the high altitude of energy input minimizes surface level feedbacks, and high-level cloud cover is reduced. With a more realistic increase of stratospheric water vapor of 7%, the middle atmosphere cools by 0.5°C or less, and the surface temperature change is neither significant nor consistent. Overall, the experiments emphasize that stratospheric changes affect tropospheric dynamics in the model, that tropospheric changes can affect stratospheric dynamics, and that tropospheric feedback processes and natural variability are important when assessing the climatic response to aircraft emissions.

1. Introduction

Both subsonic and supersonic aircraft emissions include constituents with the potential to alter the local and global climate. Species important in this respect include water vapor, NO_x (through its impact on O_3), sulfur, soot, cloud condensation nuclei, and CO_2. However, the aircraft perturbations for most of these cannot yet be tightly constrained. Therefore any evaluation must be general, with a quantitative evaluation given for a specific magnitude of forcing, to be readjusted when better estimates of the emissions impact become available.

Increases of CO_2 and water vapor and alterations of ozone and cirrus clouds have the potential to alter in situ and global climate by changing the infrared (greenhouse) opacity of the atmosphere. Sulfuric acid, which results from sulfur dioxide emissions may cool the climate through scattering of incoming solar radiation, while soot has both longwave and shortwave radiation impacts. The greenhouse effect of radiative constituents is largest for emissions in the upper troposphere and lower stratosphere, where the effectiveness is amplified by the colder radiating temperatures. In addition, large residence times and low background concentrations may further enhance the impact of aircraft emissions.

In this paper we concentrate on the potential climatic and dynamical impacts of ozone and water vapor perturbations

[1]Hughes/STX Corporation, New York.

Paper number 95JD00196.
0148-0227/95/95JD-00196$05.00

associated with aircraft, both for the troposphere and for the stratosphere. The dynamical changes are important, for they may influence assessments of the how aircraft will influence ozone and water vapor concentrations. We use the Goddard Institute for Space Studies global climate/middle atmosphere model (GISS GCMAM) [*Rind et al.*, 1988a, b]. This model has 23 layers in the vertical and 8° × 10° (latitude by longitude) resolution in the horizontal. It includes all the normal processes for climate models; for example, it calculates its own cloud cover and snow cover. For climate change purposes it calculates sea surface temperatures for an ocean with a maximum mixed layer depth of 65 m and specified ocean heat transports, as described by *Hansen et al.* [1984]. In the stratosphere it has parameterized gravity wave drag due to model-generated processes associated with topography, convection, and wind shear.

As discussed by *Rind et al.* [1988a], due to uncertainties in the model's cross-tropopause water vapor transport, water vapor values in the model stratosphere are specified and are not allowed to interact with the tropospheric water vapor. The water vapor above 100 mbar is specified in the control run to be 3 parts per million by mass (ppmm) everywhere; observed variations of water vapor in the stratosphere, as shown, for example, by SAGE II data [*Rind et al.*, 1993] would alter the control run temperature by at most several degrees at different latitudes and altitudes. However, the specification implies that changes in water vapor, due to altered troposphere/stratosphere exchange associated with the climate perturbations, cannot influence the results.

The experiments for each constituent are run in three phases. First, gross changes are made to the atmospheric concentrations and the model is integrated for 3 years without allowing sea surface temperatures to adjust. The resulting changes, either climatic or dynamic, are due primarily to the direct radiative perturbations associated with the altered constituent; as the atmospheric response time is of the order of a few months, these are effects that can be realized in the near term.

Next, the sea surface temperatures are allowed to adjust to radiative imbalances, in experiments which are integrated for some 20–30 years. Now the climatic feedbacks can be activated, a phenomenon which would take several decades. The differences between these two experiments illustrate the impact of the full suite of tropospheric responses on climate and dynamics.

Finally, more realistic perturbations are employed with varying sea surface temperatures, in experiments run for 20–50 years. The gross experiments allow for a clear indication of the types of changes to be expected with a large signal-to-noise ratio; the more realistic experiments produce a muted but more practical example of those changes.

Results below are shown as 3-year averages, following a spin-up, for the specified sea surface temperature experiments compared with a 10-year control run, and for the last 5 years of multidecade runs for both the control and the experiments with varying sea surface temperatures. In the experiments with altered sea surface temperatures, ocean heat transports are incorporated to help the control run look more like the current climate [*Hansen et al.*, 1984]; these transports are then unchanged in the experiments, i.e., no ocean dynamical responses are included.

2. Ozone Perturbations

The impact on the net surface radiation of ozone perturbations depends on the vertical distribution of the ozone change. Reduction in tropospheric and lower stratospheric ozone tends to cool the climate, by reducing the atmospheric greenhouse capacity. Reduction in middle and upper stratospheric ozone tends to warm the climate, by allowing more shortwave radiation to reach the surface [*Lacis et al.*, 1990]. The results also depend somewhat on latitude, season, and the vertical temperature profile. For example, upper stratospheric ozone reduction is obviously less efficient in warming the surface at high latitudes during winter, and the greenhouse effect is amplified in the tropics, where the difference between the surface and the lower stratospheric air temperatures is largest.

The preliminary assessments of the NASA Atmospheric Effects of Stratospheric Aircraft (AESA) High-Speed Research Program (HSRP) [1993a, b] are that subsonic and supersonic transports could decrease ozone in most of the stratosphere by a few percent, while increasing it in the tropical lower stratosphere and upper troposphere by a similar percentage. The tropospheric results are somewhat uncertain, since the two-dimensional models used to produce them have not been validated for tropospheric chemistry.

In fact, a wide range of estimates for the troposphere exist. Using the database of NO_x emissions from subsonic aircraft provided by *McInnes and Walker* [1992], *Sausen and Kohler* [1993] calculated with a three-dimensional model that the background concentrations of nitrogen oxides from 40° to 60°N could have increased by 30–100%. The effect on ozone of such subsonic aircraft emissions has been investigated by *Johnson et al.* [1992] and *Beck et al.* [1992] using two-dimensional transport-kinetics models. The studies find that the present emissions from aircraft cause an increase in ozone in the upper troposphere from 4 to 15%. F. Rohrer et al. (personal communication, 1993), using a two-dimensional transport model for a latitudinal belt between 40° and 50°N, concluded that a 4% ozone increase would occur at cruise altitudes, with little change in the lower troposphere. Here too the altitude at which the ozone change occurs is important, for tropospheric forcing far from the surface is less effective in initiating the positive feedbacks associated with water vapor changes. *Hansen et al.* [1993] reported initial results from a coarse resolution sector general circulation model (GCM) of the influence of ozone changes at various altitudes on the surface air temperature; doubling tropospheric ozone at altitudes below 7 km (400 mbar) increases surface air temperature by 0.6°C. The actual climatic impact of aircraft-induced ozone changes will depend upon accurate reconstructions of the ozone perturbations between the surface and 30 km.

Hansen et al. [1993] concluded that the radiative forcing associated with stratospheric ozone changes was not simply translatable into a surface air temperature response, as is the case for CO_2 or solar forcing. The restricted vertical structure of the ozone perturbation (i.e., at specific altitudes in the stratosphere) results in an alteration in the temperature lapse rate, in violation of the assumption of the one-dimensional radiative-convective models used to convert radiative forcing into surface temperature response. The magnitude of the surface air temperature response (in °C/W

m^{-2}) depended critically on the level of constituent change, with greater response when the perturbation was close to the surface, and therefore capable of inciting feedbacks associated with surface forcing (e.g., evaporation-water vapor changes, snow/ice albedo feedback).

The following experiments with the GCMAM are a further attempt to quantify the climatological impact of ozone changes. As indicated above, the first experiments are with large ozone changes, initially without allowing sea surface temperatures to change, then with the full thermodynamic response of the system. The last experiment uses a "more realistic" perturbation associated with aircraft emissions.

2.1. No Ozone in Lower Stratosphere, Specified Sea Surface Temperatures

In the first ozone experiment we amplify the ozone reduction capability of stratospheric aircraft by removing all ozone from the lower stratosphere, between 200 and 50 mbar (approximately 12 to 20 km in altitude). (The actual change in ozone can be determined by reference to the control run ozone distribution, shown in Figure 8a). The resulting annual change in temperature is shown in Figure 1. The primary impact on the annual average is a strong cooling of the lower stratosphere by up to 10°C at tropical latitudes and about half that much at the poles. This effect is primarily due to the loss of infrared absorption, although solar heating rates decrease by more than 0.1°C d^{-1} at low latitudes and close to 0.3°C d^{-1} near the poles. The tropospheric temperatures are essentially unchanged. Global surface air temperatures cool by only 0.03°C due to the specification of fixed sea surface temperatures; surface air temperatures over land cool by 0.2°C. As the interannual standard deviation is 0.04°C for the global surface air temperature and 0.075°C over land with unchanging sea surface temperatures, only the change over land is significant.

In the middle stratosphere, temperatures warm by a few degrees in the tropics and at midlatitudes in both hemispheres, while at the pole there is cooling in the northern hemisphere and reduced warming in the southern hemisphere. Removal of lower stratospheric ozone has allowed middle stratospheric ozone to absorb longwave radiation from below, with the effect maximizing at low latitudes where the upwelling radiation is the greatest.

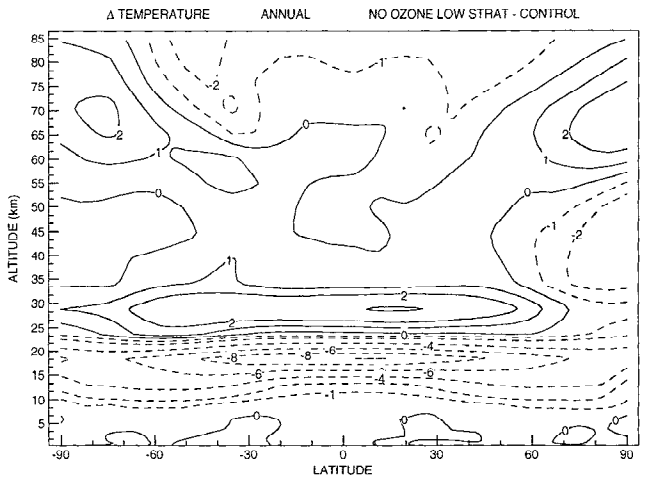

Figure 1. Model-produced annual average temperature change between the experiment with all ozone removed from the lower stratosphere (from 200 to 50 mbar) and the control run. Results are for 3-year averages for the experiment, 10-year averages for the control run. Sea surface temperatures were not allowed to change.

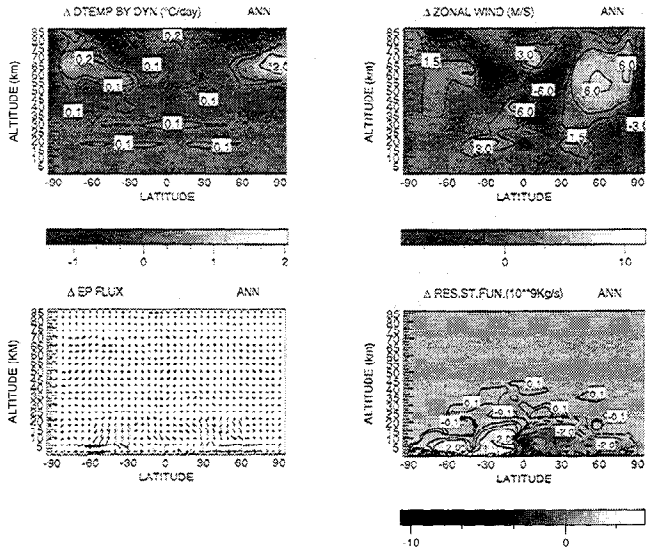

Figure 2. Annual average changes between the experiment with no ozone in the lower stratosphere and the control for difference in dynamical heating rates (top left); difference in zonal winds (top right); difference in Eliassen-Palm (E-P) flux (bottom left); difference in residual stream function (bottom right).

This latitudinal gradient in heating is one of two factors which lead to altered dynamical heating rates (Figure 2, top left), which further modify the temperature response. There are some differences in the dynamical responses between the hemispheres, so we concentrate on the northern hemisphere first. The increased latitudinal temperature gradient generated by the radiative response gives rise to an increase in zonal winds in the stratosphere, from 30° to 60°N (Figure 2, top right). In response, there is less vertical propagation of wave activity, as indicated by a reduced vertical E-P (Eliassen-Palm) flux (Figure 2, bottom left). Less wave energy therefore enters the upper stratosphere and mesosphere; for example, the region from 10 to 0.5 mbar has 5% less eddy energy. As eddies in the control run largely act to intensify the residual circulation and decelerate west winds at these levels, the reduced energy leads to a reduction in the middle to upper stratosphere residual circulation of about 10%, polar dynamical cooling of the order of 0.2°C d^{-1}, and an increase in zonal winds throughout the higher levels.

While less energy is propagating out of the lower stratosphere into regions above, more is propagating in from below, leading to an overall increase in lower-stratospheric eddy energy of about 10%. Tropospheric baroclinic eddy energy generation and eddy energy itself increases, by up to 10% at middle latitudes; this is the result of increased eddy available potential energy, associated with the colder lower stratosphere and hence decreased vertical static stability. More energy then propagates upward through the 100-mbar level (by about 10%), leading to greater E-P flux convergence and an accelerated residual stream function (by about 10%) in the lower stratosphere (Figure 2, bottom right). The altered dynamics produces an increase in dynamical heating

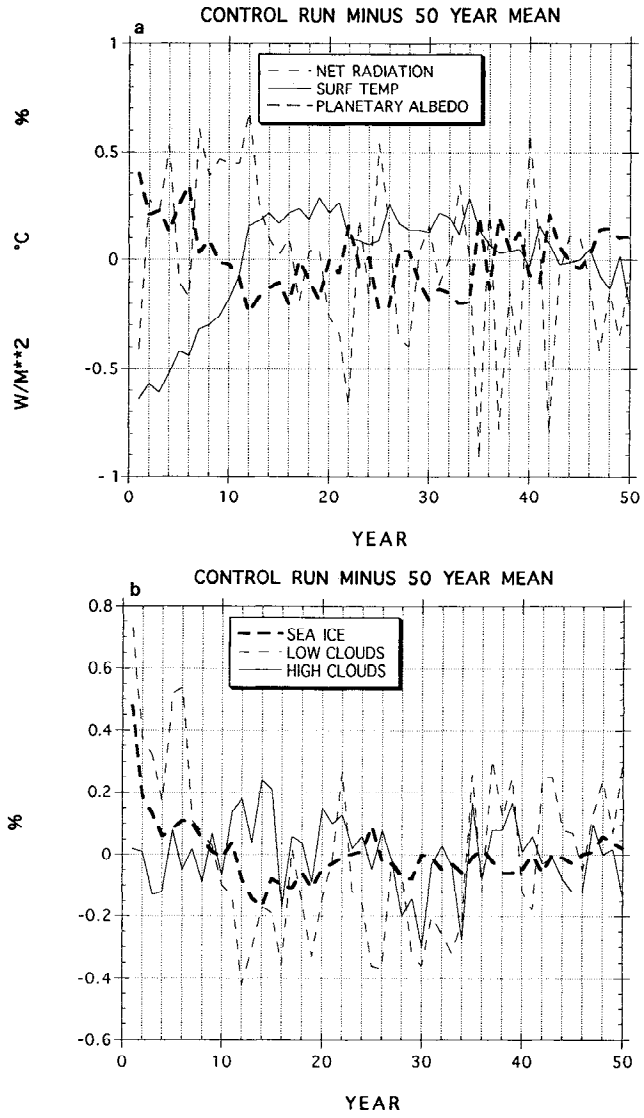

Figure 3. Variation of annual, global average values in the current climate control run relative to the 50-year mean. (a) Net radiation at the top of the atmosphere; surface air temperature; planetary albedo. (b) Sea ice cover, low clouds (940–800 mbar); high clouds (500–100 mbar).

of the lower stratosphere and middle stratosphere, by about 0.1°C d^{-1}, offsetting some of the radiative cooling in the lower stratosphere and amplifying the radiative warming in the middle stratosphere.

The increased stratospheric winds have an additional effect, on the parameterized gravity waves in the model, which influences the stratosphere and mesosphere. The stronger winds in the middle and upper stratosphere increase the required mountain wave saturation flux in the model, hence the parameterized mountain gravity waves undergo less breaking and less momentum damping there (a positive feedback further amplifying the zonal winds). The parameterized waves thus propagate to higher altitudes and accelerate the residual circulation in the mesosphere, producing increased dynamical warming of up to 2°C d^{-1} near the pole (Figure 2, top left). The increased damping effect of the mountain waves in the mesosphere is about 20% of the decreased wind acceleration being done by the large-scale dynamics at that altitude, due to the reduced eddy energy. The rest of the mesospheric momentum balance is made up by increased (parameterized) shear wave-induced deceleration, with increased shear wave generation associated with the stratospheric west wind increase. The general mesospheric cooling (outside of the region of polar warming) is associated with the increased residual circulation driven by the greater gravity wave drag.

The southern hemisphere also experiences increased eddy energy propagating through the tropopause, but in addition there is increased energy flux into the higher levels of the middle atmosphere. This is consistent with the more uniform temperature warming with latitude in the middle stratosphere and the more moderate stratospheric wind increase in that hemisphere. The difference appears to be associated with the basic differences in longwave-generating capability between the two hemispheres. In the northern hemisphere there is greater topography at upper middle latitudes and greater vertical E-P fluxes through the tropopause in the control run. Thus when this energy increases, its influence on accelerating the residual circulation extends to the pole. In the southern hemisphere the increased energy flux through the tropopause is not as large poleward of 50° latitude, hence the residual circulation increase, which acts to accelerate the lower-stratospheric west winds (by advecting the large tropical cooling, from the ozone depletion, poleward and thus cooling high latitudes) does not reach as far. The southern hemisphere thus is warmer at high latitudes in the middle stratosphere, and the increased energy from below can propagate more effectively to higher levels.

2.2. No Ozone in Lower Stratosphere, Calculated Sea Surface Temperatures

In this experiment, sea surface temperatures are allowed to change, in both the control and the perturbation runs. The control run variations in relevant parameters are presented in Figures 3a and 3b, compared to the 50-year mean. The surface air temperature and several of the other parameters undergo some change during the first decade, then fluctuate around the mean without any obvious trend. All time-averaged differences between experiment and control will be for years during which the control run simulation was stable.

How is the climate altered when ozone is removed from the lower stratosphere and sea surface temperatures are allowed to adjust? The variation of the relevant climate parameters with time is given in Figures 4a and 4b. The surface air temperature has decreased more than 1°C associated with the reduction in atmospheric greenhouse capacity due to the ozone loss. Positive feedbacks include an increase in sea ice cover and low-level clouds, while the increase in high-level clouds is a negative feedback. Note that the changes in temperature, sea ice, and high clouds are highly significant, amounting to more than three standard deviations of the control run values (Figures 3a and 3b). The net radiation at the top of the atmosphere, which indicates how close the model is to radiation balance, is close to zero, indicating that if the experiment were run longer, the additional temperature change would be small.

Table 1 shows the changes in climate parameters of interest averaged over the last 5 years of the experiment. Also shown are the interannual standard deviations in the control run. The changes are generally 5 to 10 times the interannual standard deviations and thus highly significant.

With the proper caveats we can relate these changes to the resulting surface air temperature response. By comparison with *Hansen et al.* [1984] and *Pollack et al.* [1993] we crudely estimate that the planetary albedo change produces a cooling of approximately 0.3°C, of which about 0.1°C is due to the increase in snow cover and sea ice. The water vapor reduction should lead to a cooling of about 0.4°C. The radiative forcing which results from the ozone change (and lower stratospheric adjustment) can be determined from the specified sea surface temperature experiment: at the tropopause, removing all the ozone in the lower stratosphere produces a net radiation loss of about 2 W m^{-2}. This reduction is difficult to relate directly to a surface air temperature change, since the restricted level of the ozone loss alters the lapse rate (hence violating assumptions in the one-dimensional radiative-convective models used for such assessments). A very crude estimate is that it would lead to cooling of the order of 0.5°C.

The cloud cover contribution is the most intriguing, since it deviates from the results of previous experiments. As noted by *Hansen et al.* [1984], *Rind* [1986], and *Pollack et al.* [1993] the GISS GCM like other models tends to produce decreased low-level clouds with some increases in high-level clouds as climate warms and the opposite effects as climate cools. The change is related to alterations in the large-scale circulation, with some input from increased convection [e.g., *Mitchell and Ingram*, 1992]. However, in this cooling experiment, while low-level clouds do increase, upper level clouds also increase, especially at low latitudes. The change is mostly associated with increased eddy energy at altitudes above 300 mbar due to the altered stability resulting from lower stratospheric cooling. The high-level cloud change occurred in the experiment with specified sea surface temperatures (and hence no tropospheric cooling) as well, amounting to a 1.7% increase in that experiment. The cloud cover increase as a whole contributes to a larger planetary albedo, with an approximate cooling contribution of 0.2°C. However, the cloud altitude change will produce a warming tendency; to make the total radiative responses equal the observed temperature change requires a warming of a few tenths of a degree, but with the uncertainty in the ozone contribution, the effect could be larger.

The change in surface air temperature as a function of latitude is presented in Figure 5. The largest temperature change occurs in the northern hemisphere extratropics and

Table 1. Annual, Global Average Changes in Ozone Modification Experiments

Parameter	Units	Δ No Ozone	Δ Mod Ozone	s.d.
Surface temperature	°C	−1.13	0.03	0.09
Ground albedo	% absolute	0.29	−0.01	0.04
Planetary albedo	% absolute	0.86	0.07	0.07
Absorb shortwave radiation at top of atmosphere	W m^{-2}	−2.6	−0.25	0.24
Net longwave radiation at top of atmosphere	W m^{-2}	−2.5	0.10	0.21
Evaporation	% relative	−2.3	0.20	0.44
Specific humidity	% relative	−8.9	0.40	0.80
Snow cover	% relative	6.9	0.00	0.86
Sea ice	% relative	5.7	−1.80	0.73
Total clouds	% absolute	2.0	0.18	0.27
High clouds	% absolute	2.5	0.17	0.61
Low clouds	% absolute	0.5	0.11	0.50

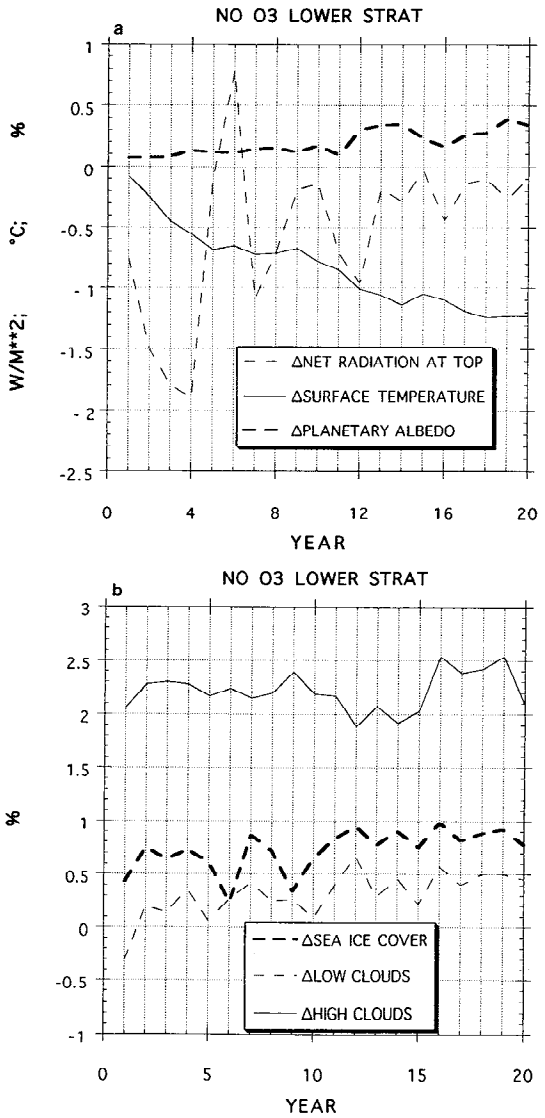

Figure 4. (a) and (b) As in Figure 3 except for the variation of annual, global average differences between the experiment with ozone removed from the lower stratosphere and the control run.

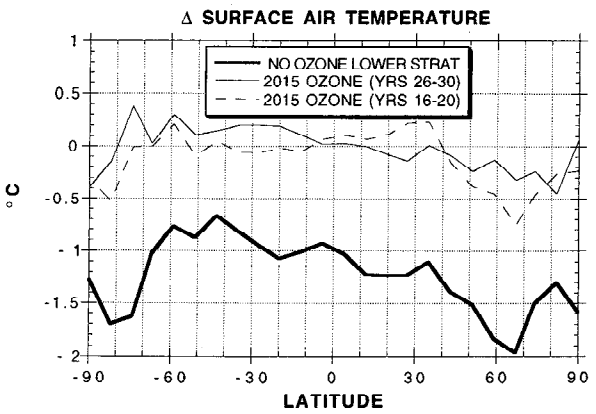

Figure 5. Surface air temperature change as a function of latitude due to ozone changes.

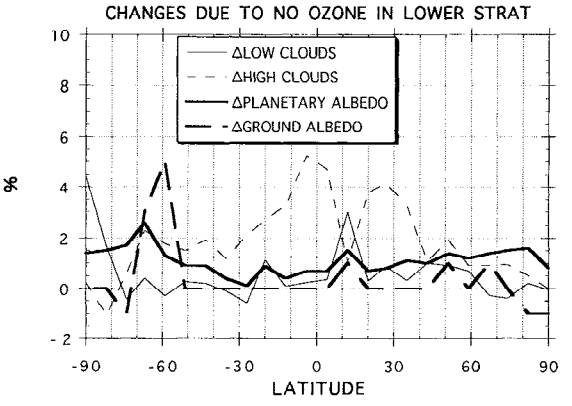

Figure 6. Latitudinal changes of climate parameters due to removal of ozone in the lower stratosphere.

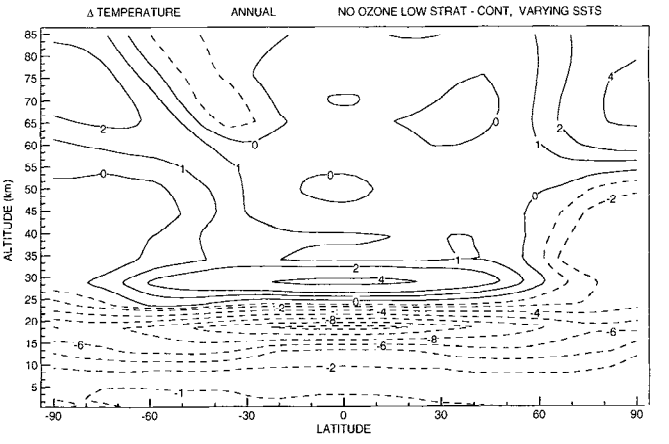

Figure 7. As in Figure 1 except the sea surface temperatures were allowed to adjust. Results are averages over the last 5 years of a 20-year simulation for the experiment and 30 years for the control run.

high latitudes of the southern hemisphere, both regions where low-level cloud cover, ground albedo (sea ice and snow cover), and planetary albedo changes are largest (Figure 6). Reduced cooling occurs at latitudes of high cloud cover increase and small planetary albedo change.

The latitude-altitude temperature response (Figure 7) is basically similar to the result without allowing sea surface temperatures to change (compare with Figure 1). Lower-stratospheric cooling is slightly intensified, since with reduced lower-tropospheric temperatures, infrared radiative flux to the stratosphere is smaller.

The changes in eddy energy which arose with specified sea surface temperatures due to the alteration of static stability occur in this experiment as well. Given in Table 2 are the percentage changes in tropospheric eddy available potential energy (EAPE), and tropospheric and lower-stratospheric eddy kinetic energy (EKE) for the two sets of experiments, as well as the interannual standard deviations. The increase in tropospheric eddy energies are 4 to 10 times the control run standard deviations, while the lower stratospheric EKE increases are even more significant. Associated transport changes are noticeable in the lower stratosphere.

The greater tropical cooling leads to a distinct decrease in stratospheric west winds in both hemispheres in the calculated sea surface temperature experiment. As can be seen in Figure 7 compared with Figure 1, another difference is that the mesosphere from 50°N to 50°S now shows slight warming. The residual circulation changes at these altitudes are smaller in this experiment due to reductions in gravity wave forcing from below and, in the southern hemisphere, reduced planetary wave energy as well. The weakened stratospheric west winds result in a smaller change in both mountain and shear wave drag in the mesosphere, muting their driving of additional residual circulations. The stratospheric wind changes have altered the wave refraction pattern in the southern hemisphere, so that more wave energy propagates to higher latitudes and less propagates vertically at upper middle latitudes into the upper stratosphere and mesosphere. This then further reduces the residual circulation increase at those levels. As the increased residual circulation, with upward motion throughout low and subtropical latitudes, was acting to cool these altitudes, the effect has largely disappeared in this experiment.

2.3. More Realistic Ozone Changes From Aircraft Emissions

Having established the basic tendencies of the model response to ozone depletion in the stratosphere, we now utilize the ozone changes estimated from potential aircraft emissions by the year 2015 [*IISRP/AESA*, 1993a]. In particular, we chose the annual average changes associated with 500 supersonic aircraft flying at Mach 2.4, NO_x emission index (EI) = 15 with modified subsonic schedules, as determined by the two-dimensional Goddard Space Flight Center (GSFC) photochemistry model, which is representative of results from other models. The input ozone changes are given in Figures 8a and 8b. The tropospheric changes are uncertain, since the photochemistry model has not been validated for the troposphere.

The experiment using this ozone perturbation was integrated for 30 years, allowing the sea surface temperatures to adjust. At the surface, stratospheric ozone reduction leads to reduced downward infrared radiation; however, ozone reductions at upper levels also allow more sunlight to reach the surface, providing a warming tendency. Furthermore, since tropical upper tropospheric ozone is increased, this also has the effect of warming the surface. Therefore the surface temperature is responding to these minimal and conflicting tendencies.

Given in Figures 9a and 9b are the changes in global average temperature and the relevant climate parameters as a function of time. Averaged over the last 5 years of the experiment, the global surface air temperature warms by

Table 2. Percentage Change in Annual, Global Average Eddy Energy Values for "No Ozone in Lower Stratosphere" Experiments

Experiment	Trop EAPE	Trop EKE	100- to 50-mbar EKE
Specified SSTs	4.1	3.1	23.3
Calculated SSTs	7.1	6.0	21.9
s.d.	0.7	1.2	1.5

Trop EAPE, tropospheric eddy available potential energy; EKE, eddy kinetic energy.

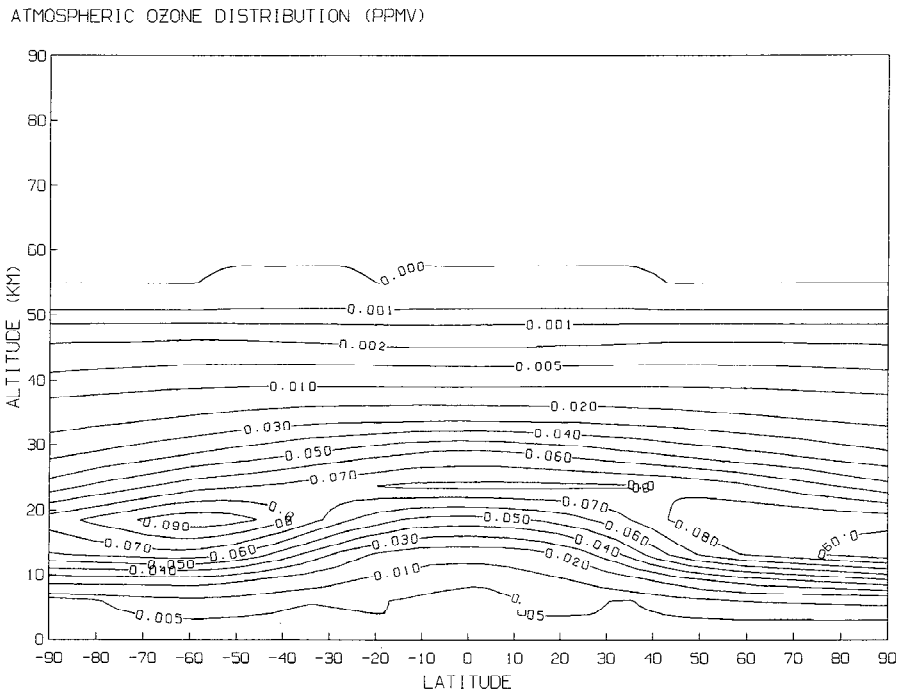

Figure 8a. Ozone concentrations (ppmv) used in the control run [from *McPeters*, 1993].

0.025°C; comparison with the interannual standard deviations in Table 1 shows that this change is not significant and, in fact, Figure 9 shows as many years with small temperature decreases as with a temperature increase. The feedbacks also alternate in sign. A similar comparison for the other climate parameters show that the other global changes are not significant either.

The latitudinal variation of surface air temperature change is shown in Figure 5, and the change in associated parameters of climatic interest are given in Figure 10. Figure 5 shows values of the surface air temperature for the "realistic" ozone change during two time slices: years 16–20, when the global average temperature was decreasing by 0.02°C, and years 26–30, when it was increasing by a similar amount. Despite this difference the pattern of temperature change with latitude is fairly similar, and also fairly similar to that with complete ozone removal in the lower stratosphere. The reason for this consistency in pattern is found in the similarity of the forcing (ozone removal) and the feedbacks. Comparing Figures 6 and 10, one can see that cooling is again greatest where low-level clouds, ground albedo (sea ice and snow cover), and the planetary albedo increase is largest, and warming or reduced cooling occurs where high clouds increase or low-level cloud cover decreases. The amplified cooling at high latitudes is associated with the presence of sea ice and its ability to respond to reduced infrared forcing (note in Figure 8 that the ozone changes are all negative at the higher latitudes), reduced tropospheric eddy transports (see below), and the distance from the tropical high cloud cover increase. Thus even though the global average changes are variable and not significant, a relatively stable pattern of response is visible when the latitudinal structure is considered.

The latitude-height temperature changes are given in Figure 11 for the two time periods discussed above, one with lower-tropospheric warming (years 26–30) and the other with lower-tropospheric cooling (years 16–20). As the ozone perturbations are small, so are the corresponding temperature changes; where the patterns for the two time periods are similar, the results are more likely to represent a stable model response. Note that these results are equilibrium simulations and would not be expected to occur at the year 2015 (the time lag to reach equilibrium would probably be of the order of 30–40 years, considering the ocean mixed layer primarily).

The cooling in the tropical stratosphere is the result of both infrared and shortwave affects; solar heating decreases by 0.004°C d^{-1}. Comparison of Figures 8 and 11 indicates that the tropical cooling actually extends down into the regions of ozone increase, an infrared effect from the cooling above since neither the solar heating nor the dynamics is causing cooling there.

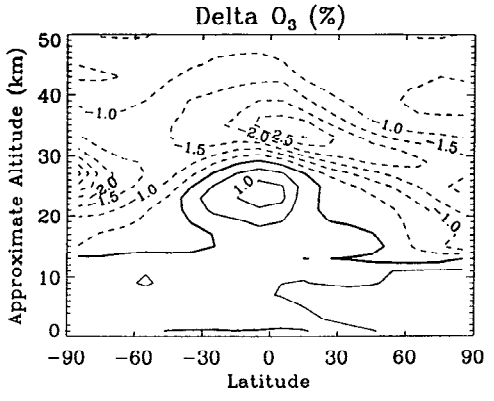

Figure 8b. Input changes in ozone due to aircraft perturbations for the year 2015 [from *HSRP/AESA*, 1993a; R. Stolarski, personal communication, 1994].

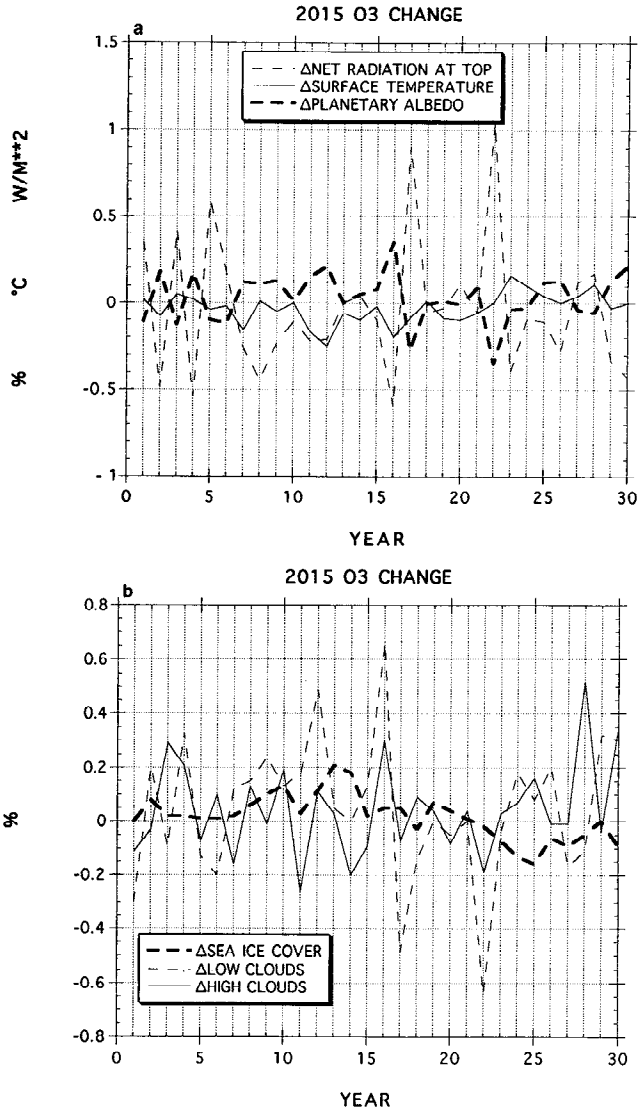

Figure 9. (a) and (b) As in Figure 3 except for difference between the "realistic" aircraft-induced ozone changes and the control run.

Dynamical warming occurs in the polar lower and middle stratosphere in the northern hemisphere, with dynamical cooling above. These changes are associated with an E-P flux convergence and residual circulation increase/decrease in the stratosphere/mesosphere. Peak stratospheric changes are of the order of 8%. The cause of these changes is similar to that of the other ozone reduction experiments, increases in northern hemispheric tropospheric and lower-stratospheric longwave energy with the reduction in static stability due to middle atmospheric cooling, especially for waves with the largest vertical wavelengths (primarily wavenumber 1). Reduced winds in the extratropical stratosphere result in increased mountain wave breaking at stratospheric levels and decreased parameterized shear waves, both effects which result in decreased gravity wave forcing of the residual circulation in the mesosphere and polar cooling.

For shorter wavelength waves the warming of the northern hemisphere lower stratosphere increases the tropospheric stability, reduces tropospheric eddy energy and eddy transports in the middle troposphere, and contributes to the extratropical cooling. Thus Figure 11 presents overlying regions with changes of alternating sign, all related to dynamical interactions.

3. Water Vapor Perturbations

Water vapor is the primary atmospheric greenhouse gas. Increases in water vapor associated with aircraft emissions have the potential to warm the climate, while producing cooling at altitudes of release, due to greater thermal emission. The effects are largest when water vapor perturbations occur near the tropopause [*Grassl*, 1990; *Rind and Lacis*, 1993], as is likely to be the case from supersonic emissions.

High-speed aircraft may increase stratospheric water vapor by up to 0.8 ppmv for a broad corridor at northern hemisphere midlatitudes, with a global average effect perhaps ¼ as large. In a one-dimensional model analysis, increases in stratospheric water vapor of 3 ppmv produced a global average warming of 0.6°C [*Rind and Lacis*, 1993]. Were this assessment correct, since perturbations of this magnitude are essentially linear, the estimated change due to supersonic aircraft alone would provide surface warming of the order 0.1°C.

Schumann [1994] estimated that subsonic tropospheric emissions of water vapor may well be of the order of 0.02 ppmv over the North Atlantic flight corridor and 0.002 ppmv if mixed uniformly over the troposphere with a lifetime of 9 days. *Shine and Sinha* [1991] estimate that a global increase of 1 ppm for a 50-mbar slab between 400 and 100 mbar would increase surface air temperature by 0.02°C. Therefore future subsonic emissions of water vapor would have to be substantially increased to have a noticeable impact on surface temperatures.

These analyses have been carried out with one-dimensional or otherwise simplified models. Experiments with the GCMAM were conducted to obtain a three-dimensional assessment, with the possibility of interactive feedbacks. The experiments followed a procedure similar to that for ozone: a large perturbation was input to the stratosphere without allowing the sea surface temperatures to change to gauge the response due to the in situ effects; then sea surface temperatures were allowed to adjust, to assess the impact of the feedbacks and tropospheric response. Finally a "more realistic" aircraft perturbation was employed, with the full sea surface temperature response.

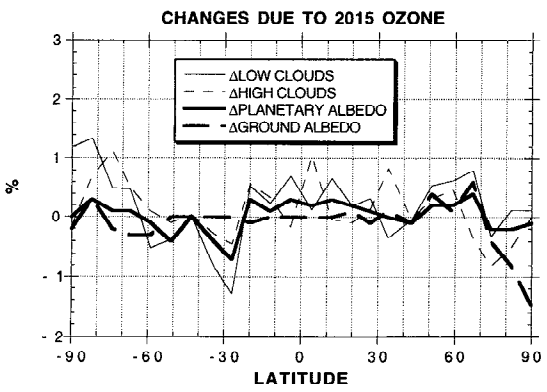

Figure 10. Changes of climate parameters due to 2015 ozone changes for years 26–30.

3.1. Doubled Stratospheric Water Vapor With Specified Sea Surface Temperatures

Middle atmosphere water vapor values were doubled, from 3 to 6 ppmm, above 100 mbar. The annual average temperature changes associated with this increased water vapor are shown in Figure 12. As expected, the middle atmosphere cools by 2°–3°C at most latitudes and levels, somewhat less at high latitudes and at low levels in the stratosphere. This cooling is associated with the greater infrared radiating capability of the stratosphere due to the presence of the increased water vapor, which exceeds the small increase in shortwave absorption (of 0.1°–0.2°C d^{-1}). The upper troposphere warms in most regions, from absorption of the increased downwelling thermal radiation. (As noted, stratospheric water vapor values are specified and not advected. Therefore the addition of water vapor to the stratosphere in these experiments does not change the tropospheric water vapor loading. Given the small values of the additional stratospheric water vapor, the change would not affect the tropospheric humidity in general, although it could have a noticeable effect in the upper troposphere; 3 ppmm is about 15% of the model's upper troposphere (150 mbar) water vapor in the tropics.)

The reduced cooling in the lower stratosphere is largely a radiative effect, associated with increased radiation absorption from the warmer upper troposphere and due to the increased radiative capacity of these levels of temperature minima. The decreased cooling at high latitudes in the stratosphere is a dynamical effect. With decreased vertical

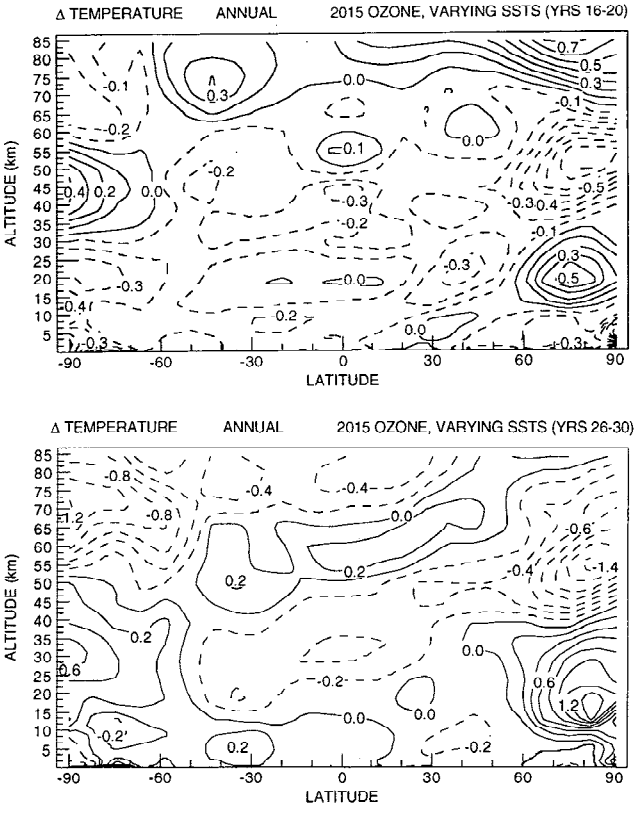

Figure 11. Model annual average temperature changes due to the ozone perturbations given in Figures 8a and 8b, with sea surface temperatures allowed to adjust. Results are for years 16–20 (top) and 26–30 (bottom).

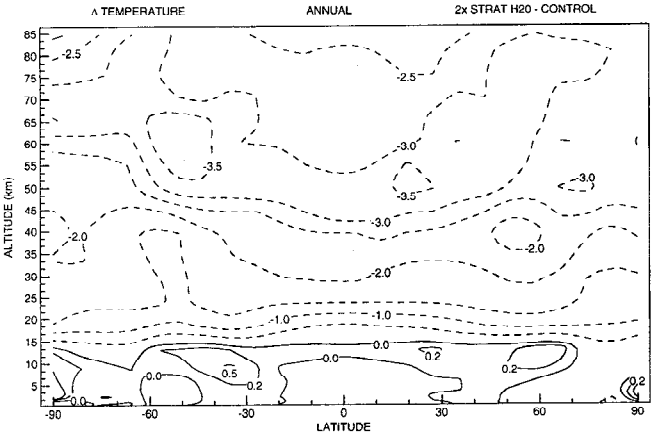

Figure 12. Model annual average temperature changes due to doubling stratospheric water vapor above 100 mbar. Results are for 3-year averages for the experiment, 10-year averages for the control run. Sea surface temperatures were not allowed to change.

stability, due to the cooler stratosphere, longwave energy increases somewhat in the troposphere. In the northern hemisphere, tropospheric wave 1 available potential energy increases by 8% and wave 1 kinetic energy increases by 13% at midlatitudes. By the midstratosphere, for the hemisphere as a whole, planetary wave 1 energy has increased by 17%, while in the southern hemisphere there is about a 10% increase in the energy of planetary waves 1 and 2 (with the change in wave 2 being somewhat larger). Increased planetary wave energy associated with a colder stratosphere also occurred in this model in the doubled CO_2 experiments discussed by *Rind et al.* [1990].

Associated with the larger planetary longwave energy, there is some increase in wave forcing (E-P flux convergence) above 10 mbar, reaching 10% or more of control run values in the mesosphere. The residual circulation in the stratosphere increases by about 5% in each hemisphere, resulting in increased dynamical warming (of the order of 0.1°C d^{-1}) at high latitudes (and greater in the mesosphere), reducing the total cooling there (Figure 12). The relevant dynamical changes are presented in Figure 13.

With the specification of the sea surface temperatures the tropospheric response is muted; surface air temperatures increase by only 0.03°C globally, 0.06°C over land. Tropospheric eddy energy overall (considering all wavenumbers) shows little change. However, the radiative warming of the upper troposphere leads to an increase in tropospheric stability at low latitudes and a reduction in Hadley Cell intensity of some 10%. Hence rainfall decreases in the tropics, and increases in the subtropics, of 5–10% arise.

3.2. Doubled Stratospheric Water Vapor, Calculated Sea Surface Temperatures

The change with time of the surface air temperature and relevant climate parameters is given in Figures 14a and 14b. While there is some variation during the early portion of the experiment, over the last 15 years a global average warming of a few tenths of a degree is evident. This value is only of the same order as the standard deviation of the model's interannual variation (Figure 3a), and the experiment and control would have to be integrated for a substantially longer

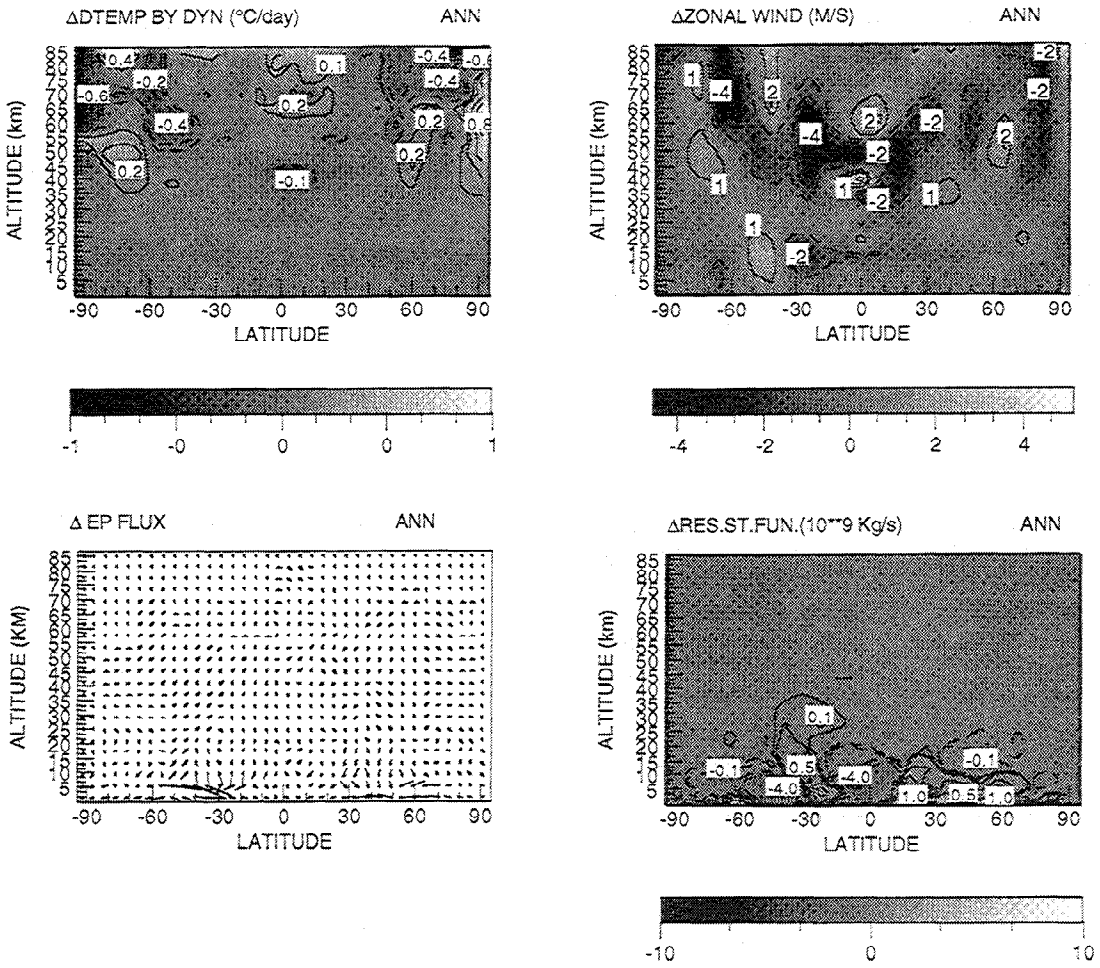

Figure 13. As in Figure 2 except for doubled stratospheric water vapor minus the control.

period of time to determine its significance. Nevertheless, the experiment is warmer than the control for 25 of the 30 years; if the yearly temperatures were independent of each other, this would happen by chance less than 0.2% of the time. Yearly climatic anomalies are not likely to be independent, since some aspects of the system (e.g., the ocean mixed layer) have time constants of greater than 1 year. Therefore we cannot determine conclusively that the additional stratospheric water vapor, in fact, leads to increased surface air temperatures. The expectation, of course, is that such warming would take place associated with the increased greenhouse forcing. During the years of the experiment in which warming occurred, the sea ice decrease provides a positive feedback, and the high-level cloud cover decrease is a negative feedback.

The global average values averaged over the last 5 years are presented in Table 3. Comparison with the standard deviations shown in Table 1 indicates that the surface air temperature change and some of the feedbacks (tropospheric water vapor and snow/ice changes) are probably significant, but on the global average, the cloud cover and albedo changes are not. Nevertheless, as shown in Figure 14b, the reduction in high-level clouds is generally consistent throughout the course of the experiment.

Doubled stratospheric water vapor increases the net radiative forcing at the tropopause by a little less than 1 W m^{-2}. If the standard translation of surface temperature response to tropospheric forcing in the GISS model of approximately 1°C/W m^{-2} were to hold, we would expect warming of the order of 0.5–1°C. Instead, the model produces warming only about 30% as large. This result is roughly consistent with the conclusion of *Hansen et al.* [1993], who found that a "ghost" forcing applied to the lower stratosphere produced about 20% of the response of the same forcing applied to the lowest model layer. There are two issues involved. The evaluation of the direct influence of radiative perturbations at the tropopause on the surface air temperature is conducted with one-dimensional radiative-convective models which assume no change in temperature lapse rate when feedbacks are not occurring. Therefore any net forcing at the tropopause affects temperatures at all levels similarly. However, the previous experiment with specified sea surface temperatures shows that this is not the case: increased stratospheric water vapor actually warms the upper troposphere radiatively, in preference to lower levels of the atmosphere. Thus the atmospheric lapse rate actually decreases; that is, warming at the surface is less than warming aloft.

Furthermore, the feedbacks which depend upon surface warming are not activated efficiently; using the same relative magnitudes discussed earlier for the ozone change experiments, we estimate that the planetary albedo change would result in surface air temperature warming of about 0.03°C, due to the sea ice and snow cover response and some cloud

cover reduction. The water vapor increase would produce warming of about 0.1°C. The water vapor response is only about 30% of what would be expected from linear extrapolation of the doubled CO_2 experiments [*Hansen et al.*, 1984], as is the ground albedo response.

The cloud altitude change works in the opposite direction: high clouds are showing a greater reduction than low clouds, diminishing the atmospheric greenhouse capacity. By analogy with the doubled CO_2 experiment, whose high-cloud decrease was 50% greater than in this run, we estimate that the reduction in effective cloud height produces a cooling of the order of 0.06°C. That would leave the doubled stratospheric water vapor direct effect producing a warming of about 0.17°C. Note that the forcing at the tropopause is roughly 40% of the "no ozone in the lower stratosphere" forcing, while the surface air temperature response is of the order of 35% of that roughly ascribed to the ozone change direct forcing.

The high clouds are slightly reduced in this experiment, while in the ozone reduction experiment, high clouds increased. When discussing that run, we indicated that the high-level increase was associated with increased eddy kinetic energy in the upper troposphere, a result of reduced vertical stability. In this experiment there is reduced stability as well, although the changes are not nearly so large: with no ozone reduction the lower stratosphere cools by 13°C (Figure 7), while with doubled stratospheric water vapor, it cools by 1°C (see Figure 17, below). Actually, clouds do increase slightly (by 1%) at the highest-tropospheric levels (200–100 mbar), but from 500–200 mbar, there is a general decrease. This response is the result of the direct radiative warming of the upper troposphere. (Note that the ozone decrease experiments result in less infrared radiation being transmitted to the upper troposphere, and whatever increased shortwave radiation occurs is inefficiently absorbed by the atmosphere.) With a reduction in the tropospheric lapse rate, tropospheric eddy energy decreases by close to 3%, leading to a general reduction in cloud cover, including high-level clouds. In addition, the moist convective mass flux above 400 mbar decreased by close to 2%, reducing moist convective clouds and convective transport of moisture; this is occurring despite the fact that the climate is warming, which usually initiates increased convection and high-level clouds [*Hansen et al.*, 1984]. Therefore the high-level cloud cover is responding more to the effects of the direct radiative forcing from above than to the surface warming.

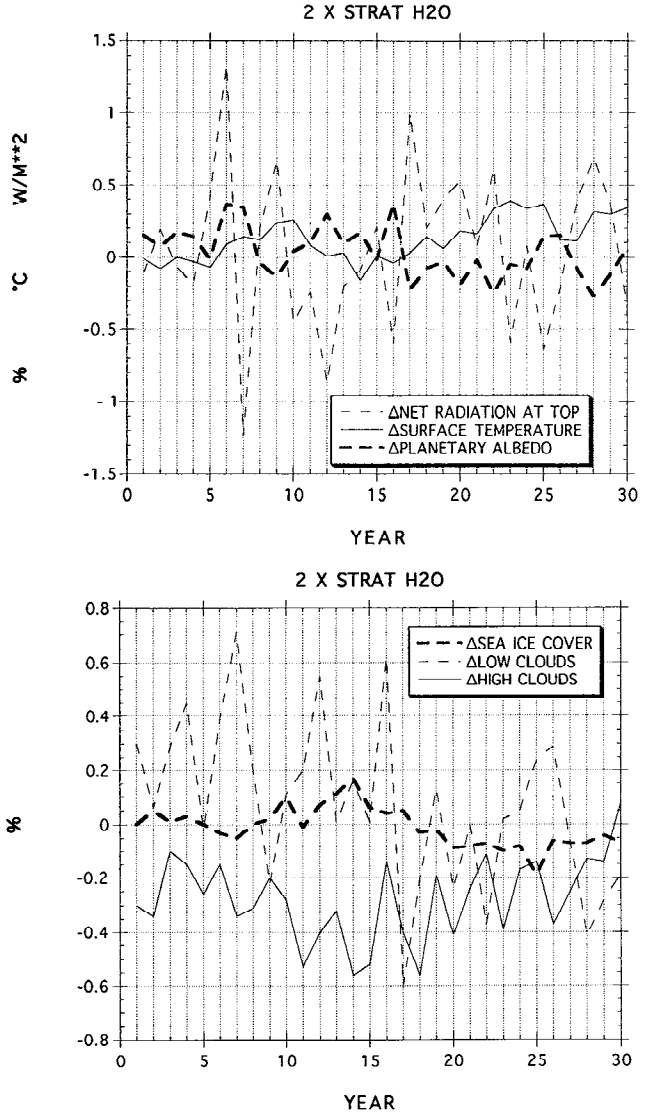

Figure 14. (a) and (b) As in Figure 3 except for the difference between the experiment with doubled stratospheric water vapor and the control run.

The variation of surface air temperature change with latitude is given in Figure 15 and the change in relevant climate parameters in Figure 16. The general reduction of high-level cloud cover has acted to diminish the warming, as has a small reduction in eddy energy transports (negative dynamical temperature changes of up to 0.04°C d^{-1} between experiments occur in the extratropics).

The latitude-height temperature changes are shown in Figure 17. With sea surface temperatures allowed to adjust, the troposphere shows somewhat greater warming (compare with Figure 12) and the stratospheric cooling is slightly greater (this latter point was true for the ozone change experiments as well; since the specified sea surface temperature runs were integrated for just three years, while the varying sea surface temperature runs went 30 years, it is conceivable that the radiative cooling was not fully complete in the specified sea surface temperature runs despite the short radiative time constant for the stratosphere as a whole).

The dynamical responses are very similar to the experiment with specified sea surface temperatures, although some details differ. For example, the tropospheric midlatitude eddy energy change in the northern hemisphere is now a wavenumber 2 phenomenon, and the lower stratosphere eddy energy change in the southern hemisphere is less purely a wave 2 phenomenon. Nevertheless, the overall patterns and magnitudes of longwave energy increase, strengthening of the residual circulation, and dynamical warming at high latitudes in the middle atmosphere are replicated. Thus though the changes are not overly large in absolute percentage in either experiment, they are consistent.

3.3. More Realistic Water Vapor Changes From Aircraft Emissions

Estimates of high-speed aircraft water vapor emissions indicate that for a flight of approximately 500 Mach 2.4

Table 3. Annual, Global Average Changes in Stratospheric Water Vapor Modification Experiments

Parameter	Units	Δ 2 X Strat H_2O	Δ 0.2 ppm Strat H_2O (26–30)	Δ 0.2 ppm Strat H_2O (46–50)
Surface temperature	°C	0.24	−0.24	0.32
Ground albedo	% absolute	−0.05	0.06	−0.11
Planetary albedo	% absolute	−0.06	0.20	−0.17
Absorb shortwave radiation at top of atmosphere	W m^{-2}	0.19	−0.68	0.59
Net longwave radiation at top of atmosphere	W m^{-2}	0.00	−0.51	−0.53
Evaporation	% relative	0.5	−1.0	1.5
Specific humidity	% relative	2.0	−1.8	2.7
Snow cover	% relative	−1.3	2.0	−1.8
Sea ice	% relative	−1.8	0	−2.4
Total clouds	% absolute	−0.04	0.29	−0.09
High clouds	% absolute	−0.16	0.07	0.03
Low clouds	% absolute	−0.05	0.35	−0.22

Strat, stratospheric.

high-speed civil transport planes (EI = 15), water vapor increases of 0.8 ppmv might occur in flight corridors, with values perhaps one fourth as large when globally averaged [*HSRP/AESA*, 1993b]. Therefore in this experiment we increased the stratospheric water vapor content from 3 to 3.2 ppmm throughout the middle atmosphere, an increase of approximately 7%. For simplicity we did not incorporate a detailed structure of water vapor change in the vertical produced by some models [*HSRP/AESA*, 1993a], nor did we allow variations associated with the specific flight paths. The water vapor increases must be viewed as tentative, considering the uncertainties in processes such as stratosphere/troposphere transport. Furthermore, we did not incorporate any changes associated with subsonic aircraft, which would impact the troposphere directly.

The forcing at the tropopause associated with this small magnitude water vapor increase is less than 0.05 W m^{-2}, hence the results would be expected to be small. The experiment (and control run) were each integrated for 50 years to better assess the significance of the results. The variation with time of the changes in global annual averaged surface air temperature and related climate parameters for the course of the experiment are presented in Figures 18a and 18b. Note the variation in sign of the surface air temperature deviations; during the last decade of the experiment, warming occurred, but through the majority of the run there was a net cooling. This can be contrasted with the situation for doubled stratospheric water vapor, in which warming almost always prevailed. The negative value of the net radiation at the top of the model at the very end of the run presages a possible return to more cooling conditions.

The relevant radiative parameters are given in Table 3 for years 26–30 and 46–50, time periods during which cooling and warming were experienced, respectively. Using the relationships given before, we estimate that the planetary albedo change would cause cooling of some 0.07°C for years 26–30 (and warming of 0.06°C for years 46–50), about one third of which is due to the snow cover increase (more than one half due to the snow cover and sea ice decrease), and the rest due to increased (decreased) cloud cover. The tropospheric water vapor decrease (increase) would lead to cooling of about 0.08°C (warming of about 0.14°C). The increase (decrease) in low-level clouds decreases (increases) the average height of the clouds; by analogy with the doubled CO_2 experiments [*Hansen et al.*, 1984] we estimate this change would cool the climate by 0.1°C (warm the climate by 0.1°C as both low clouds decrease and high clouds increase). Therefore by inference the stratospheric water vapor change

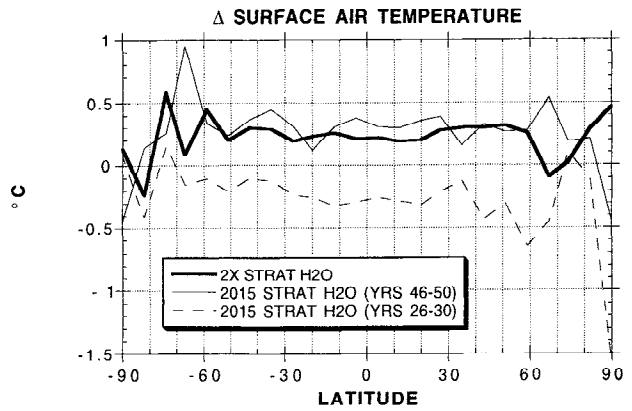

Figure 15. Surface air temperature change as a function of latitude due to stratospheric water vapor changes.

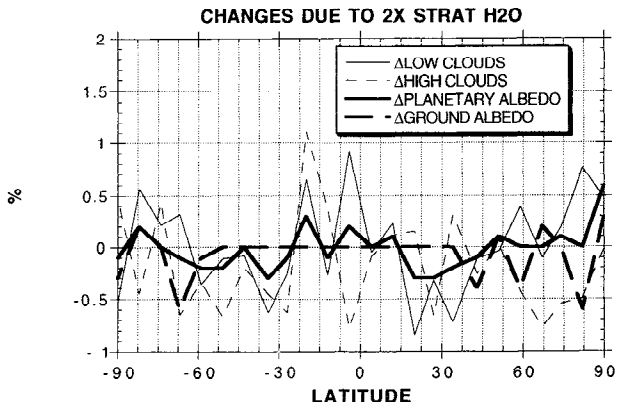

Figure 16. Changes of climate parameters associated with doubling stratospheric water vapor.

would provide direct radiative warming of about 0.01°–0.02C, about 10% of that estimated for doubled stratospheric water vapor (the water vapor increase in this experiment is 7%). As with the other estimates, there is considerable uncertainty in these numbers, not the least of which concerns the applicability of assuming linear forcings and the relevance of global averaging. Even though we have attempted to quantify these effects, the numbers should be looked upon primarily as indicating the qualitative nature of the climate forcings and feedbacks. In this case, the magnitude of the feedbacks far exceeds the direct radiative forcing.

The results in Table 3 and Figure 18 illustrate the nature of the feedbacks which dominate in this experiment. The initial tendency for the small water vapor increase is to provide for a positive net radiation balance at the top of the atmosphere, i.e., more radiation coming in then going out, initiated by the increased thermal emission from the greater stratospheric water vapor. However, the net radiation balance is dominated by the change in low clouds through the course of the experiment (compare the thin dashed curves in the two figures, noting the inverse relationship). There is a tendency in this model for a warmer climate to reduce low-level cloud cover, as increased convection and large-scale vertical motion transports moisture out of the boundary layer [e.g., *Hansen et al.*, 1984]. However, low clouds are affected by other processes (e.g., eddy energy and Hadley cell variations, evaporation in regions of sea ice change), and when the warming is only of this magnitude, variations in these other processes are of equal or greater importance. The low-cloud changes, through their impact on the planetary albedo, drive the net radiation, which governs the temperature tendency. Sea ice then responds inversely to the temperature. The same processes may be observed in the control run variations (Figure 3a and 3b). With the reduced magnitude of direct upper tropospheric warming associated with increased stratospheric thermal emission, upper level clouds no longer decrease (Table 3).

The change with latitude of the surface air temperature for years 26–30 and 46–50 are given in Figure 15. The completely different nature of the response between these sets of years is visible. The pattern of temperature change during the warmer years with the 7% increase in stratospheric water vapor is similar to that for the doubled stratospheric water

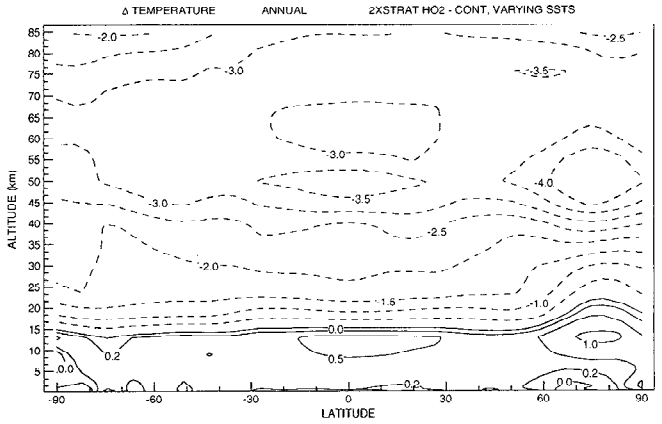

Figure 17. As in Figure 12 except sea surface temperatures are allowed to adjust. Results are averages over the last 5 years of a 30-year simulation.

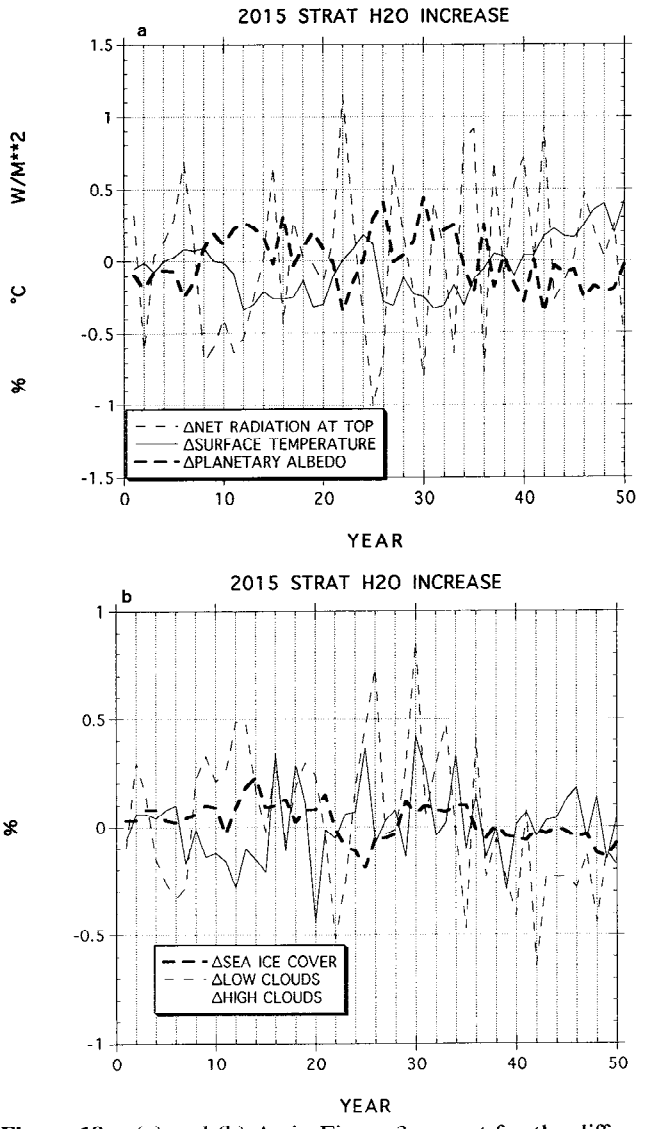

Figure 18. (a) and (b) As in Figure 3 except for the difference between the "realistic" aircraft-induced stratospheric water vapor changes and the control run.

vapor, with general warming at low and midlatitudes and increased variability at higher latitudes. The latitudinal variation of the relevant climate parameters for the warmer years is shown in Figure 19. Despite the similarity in warming the only similarity in the individual contributions (compare with Figure 16) is the decrease in ground albedo and increase in low clouds at the higher latitudes. The positive water vapor feedback (Table 3) is directly responsive to the surface warming and is thus similar in the two stratospheric water vapor experiments.

Figure 20 shows the latitude-height annual average temperature changes for the two time periods: again, common responses are more likely to indicate a robust result. As expected, the stratosphere cools, generally of the order of 0.5°C or less. The cooling is not ubiquitous: polar regions in the low to middle stratosphere warm. The warming is the result of dynamical responses similar to those seen in the prior water vapor experiments. The residual stream function increase is not quite so strong as in the doubled stratospheric water vapor experiments, and the dynamical warming is, in

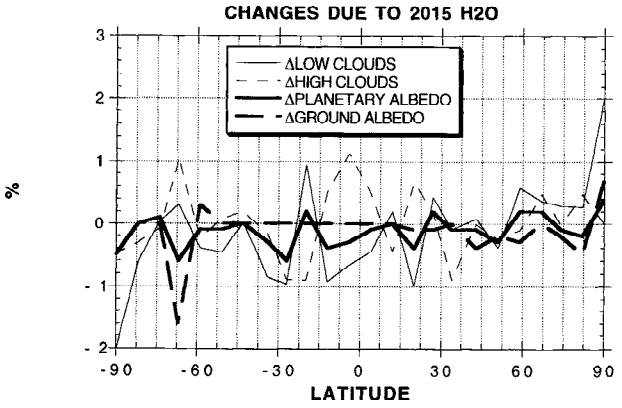

Figure 19. Changes of climate parameters associated with 2015 stratospheric water vapor.

general, somewhat less as well, although dynamical changes during the latter time period, when the tropospheric warming is in greater contrast to the stratospheric cooling, are larger than in the earlier period without this contrast. In both time periods, with the reduced magnitude of the radiative cooling increase, dynamical differences can now be larger in magnitude than the radiative perturbations, producing absolute warming. It is surprising that the dynamical perturbations were not reduced proportionately to the magnitude of the forcing; this response also occurred in experiments with this model utilizing various magnitudes of solar ultraviolet radiation changes and points to a highly nonlinear aspect of the modeled system.

4. Summary and Conclusions

The primary results of these experiments are as follows:

4.1. Ozone Experiments

1. Removing ozone between 200 and 50 mbar produces cooling in the lower stratosphere of up to 10°C and warming in the middle stratosphere about ½ as large. In the northern hemisphere the latitudinal gradient of the radiative response has the effect of increasing the stratospheric west winds, reducing eddy energy flux into the middle stratosphere and above, reducing the residual circulation there, promoting polar cooling and further west wind increases. The dynamical changes are of the order of 5–10%, with wind changes of the order of 5 ms^{-1}. In the mesosphere, increased gravity wave drag accelerates the residual circulation, resulting in polar warming.

2. The cooler lower stratosphere reduces the vertical stability for the troposphere/lower stratosphere system, and tropospheric eddy energy increases, especially for the longer waves. More energy then propagates upward through the 100-mbar level, leading to greater energy convergence and an accelerated residual stream function in the lower stratosphere, with dynamical warming. Dynamical changes are again of the order of 10%.

3. In the southern hemisphere, reduced planetary longwave activity in the control run leads to smaller changes in the zonal wind structure due to decreased ozone; therefore increased tropospheric eddy energy can propagate more easily to higher levels.

4. When sea surface temperatures are allowed to adjust, the annual, global average surface air temperature cools by 1.1°C due to the decreased downward flux of longwave energy from ozone loss, a decrease in atmospheric water vapor, and an increase in low-level clouds and sea ice. Cooling maximizes at high latitudes.

5. With the "more realistic" ozone changes estimated for the year 2015 from aircraft emissions, which involve stratospheric ozone decreases and tropospheric ozone increases, the stratosphere generally cools, up to 0.5°C. However, at the poles, stratospheric warming and mesospheric cooling arise, up to 2°C in the northern hemisphere, due to altered circulation changes associated with increased planetary wave energy (in the stratosphere) and decreased gravity wave drag (in the mesosphere).

6. The climate impact in this experiment is muted, due to the small changes and the mixed impact of decreases/increases at different levels. Overall, the global annual average surface air temperature change is not significant. However, cooling again maximizes at high latitudes where only ozone decreases are prescribed, low-level clouds and sea ice increase, and eddy energy transports and high-level clouds decrease.

4.2. Water Vapor Experiments

1. Doubling stratospheric water vapor cools the middle atmosphere by 2°–3°C while warming the upper troposphere by about 0.5°C. In the extratropics the reduced vertical stability results in tropospheric energy increases of 10% for the longest waves and similar increases in stratospheric energy; residual circulation increases of some 5% arise in

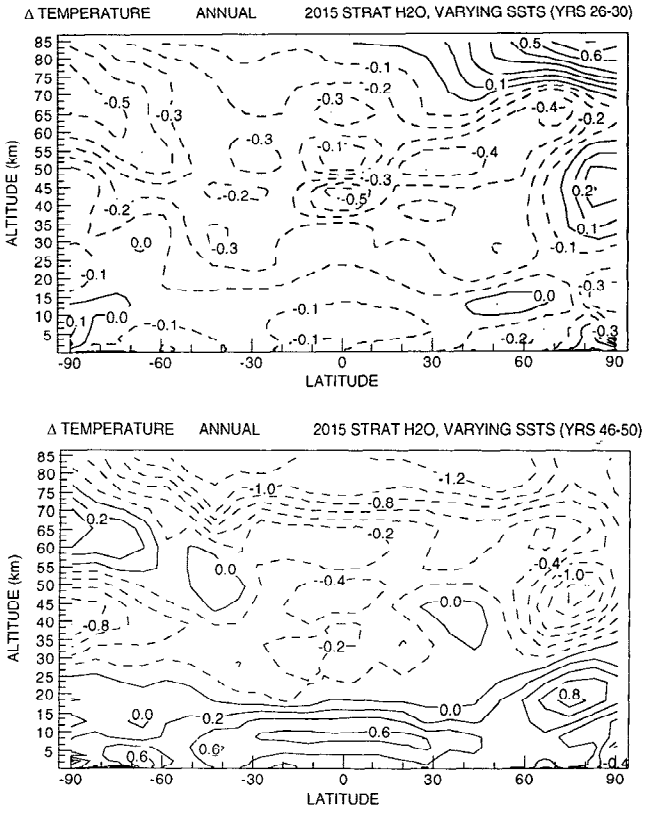

Figure 20. As in Figure 12 except for an increase in stratospheric water vapor of 0.2 ppmm. Sea surface temperatures are allowed to adjust. Results are averages for years 26–30 (top) and 46–50 (bottom).

both hemispheres (which produce changes of a similar percentage in the residual meridional winds, or a few centimeters per second on the zonal average).

2. In the troposphere the increase in tropospheric stability reduces the Hadley circulation by up to 10%, with resulting precipitation decreases in the tropics and increases in the subtropics of similar magnitude. Tropospheric zonal average meridional wind changes are up to 5–10 cm s^{-1}.

3. When sea surface temperatures are allowed to change, the dynamical responses are, in general, similar. The global, annual average surface air temperature warms by a few tenths of a degree Celsius, significantly less than expected from considerations involving water vapor-induced longwave radiation fluxes at the tropopause. The magnitude of this warming is not significant, although the experiment is almost always warmer than the control. Forcing at higher levels is by itself less efficient in impacting surface temperatures, as the lapse rate for the troposphere decreases and surface feedbacks are not well activated. In addition, the upper level warming reduces high-level cloud cover and the atmospheric greenhouse capacity, a cooling influence.

4. With the "more realistic" stratospheric water vapor increase of 0.2 ppmv due to aircraft emissions by 2015, the stratosphere cools, by 0.5°C or less, and regions of polar warming arise, associated with dynamical changes (residual circulation increases of some 5%).

5. The tropospheric changes are not consistent, as the magnitude of the feedbacks, and their inherent variability in the model, exceed the magnitude of this forcing.

The results obviously suggest that changes in the stratospheric concentration of radiatively important gases can affect the troposphere in unexpected ways. Altering the vertical stability of the troposphere/stratosphere system affects tropospheric planetary longwave energy in the model. The tropospheric dynamical responses then initiate additional radiative responses, primarily through their interaction with cloud cover generation. With the more realistic forcings used, these "secondary" responses become of equal or greater magnitude than the initial stratospheric climate perturbation. Tropospheric dynamical changes also affect middle atmospheric dynamics, altering the radiative temperature response and affecting transports.

The results also indicate the difficulties involved in simulating climate changes associated with aircraft emissions. The direct radiative forcing of these emissions is likely to be small, especially for water vapor and ozone perturbations. Given the magnitude of inherent variability in the model (and real world), very long simulations are required to determine the significance of any changes.

None of the results given here should be considered definitive. Uncertainties are associated with both the forecast changes in constituents and the model response. The tropospheric portion of the ozone change will likely receive significant attention in the coming years, and the water vapor changes are also likely to be altered. The model cloud cover response will probably be somewhat different with different cloud cover parameterizations. The tropospheric planetary longwave response may well be larger in models with greater planetary longwave amplitudes (these experiments were conducted with the coarse grid model). Spatial variations in water vapor and ozone may well occur in conjunction with specific flight paths, in contrast to the uniform distribution assumed here. Direct tropospheric insertion of aircraft emissions will further alter the vertical stability and resulting climatic/dynamical responses.

These aspects should be considered or included in future experiments dealing with the impact of aircraft emissions, which will also include other potential climatically important constituents not considered here, such as sulfur, soot, CO_2, and cloud condensation nuclei. The overwhelming conclusion from the runs conducted in this study is that given the magnitude of the proposed direct aircraft climate forcing, it is of paramount importance to consider the effect of the feedbacks when estimating the climatic/dynamic response to aircraft emissions.

Acknowledgments. We thank James Hansen for useful comments during the course of this study, and Richard Stolarski for information concerning prospective ozone changes. This work was supported by the NASA HSRP/AESA program, while stratospheric modeling is supported by the NASA Upper Atmosphere Modeling program.

References

Beck, J. P., C. E. Reeves, F. A. A. M. de Leeuw, and S. A. Penkett, The effect of air traffic emissions on tropospheric ozone in the northern hemisphere, *Atmos. Environ.*, *26*(A), 17–29, 1992.

Grassl, H., Possible climatic effects of contrails and additional water vapor, in *Air Traffic and the Environment Lecture Notes in Engineering*, edited by U. Schumann, vol. 60, pp. 124–137, Springer-Verlag, New York, 1990.

Hansen, J., A. Lacis, D. Rind, G. Russell, P. Stone, I. Fung, R. Reudy, and J. Lerner, Climate sensitivity: Analysis of feedback mechanisms, in *Climate Processes and Climate Sensitivity*, edited by J. Hansen and T. Takahashi, *Geophys. Monogr. Ser.*, vol. 29, pp. 73–91, AGU, Washington, D. C., 1984.

Hansen, J., M. Sato, A. Lacis, and R. Ruedy, Climate impact of ozone change, paper presented at the IPCC Meeting, Intergovt. Panel on Clim. Change, Hamburg, Germany, May 1993.

High-Speed Research Program/Atmospheric Effects of Stratospheric Aircraft (HSRP/AESA), The Atmospheric Effects of Stratospheric Aircraft: A Third Program Report, edited by R. Stolarski and H. Wesosky, *NASA Ref. Publ. 1313*, 413 pp., 1993a.

HSRP/AESA, The Atmospheric Effects of Stratospheric Aircraft: Interim Assessment Report of the NASA High-Speed Research Program, *NASA Ref. Publ. 1333*, 150 pp., 1993b.

Johnson, C., J. Henshaw, and G. McInnes, Impact of aircraft and surface emissions of nitrogen oxides on tropospheric ozone and global warming, *Nature*, *355*, 69–71, 1992.

Lacis, A. A., D. J. Wuebbles, and J. A. Logan, Radiative forcing of climate by changes in the vertical distribution of ozone. *J. Geophys. Res.*, *95*, 9971–9981, 1990.

McInnes, G., and C. T. Walker, The global distribution of aircraft air pollution emissions, *Tech. Rep. LR872(AP)*, Warren Spring Lab., U.K., 1992.

McPeters, R., Ozone Profile Comparisons, vol. 2, edited by M. J. Prather and E. E. Remsberg, *NASA Ref. Publ. 1291, NASA D1-D37*, 1993.

Mitchell, J. F. B., and W. J. Ingram, Carbon dioxide and climate: Mechanisms of changes in cloud, *J. Clim.*, *5*, 5–21, 1992.

Pollack, J. B., D. Rind, A. Lacis, J. Hansen, M. Sato, and R. Ruedy, GCM simulations of volcanic aerosol forcing, I, Climate changes induced by steady state perturbations, *J. Clim.*, *7*, 1719–1742, 1993.

Rind, D., The dynamics of warm and cold climates, *J. Atmos. Sci.*, *43*, 3–24, 1986.

Rind, D., and A. Lacis, The role of the stratosphere in climate change, *Surv. Geophys.*, *14*, 133–165, 1993.

Rind, D., R. Suozzo, N. K. Balachandran, A. Lacis, and G. L. Russell, The GISS global climate/middle atmosphere model, I, Model structure and climatology, *J. Atmos. Sci.*, *45*, 329–370, 1988a.

Rind, D., R. Suozzo, N. K. Balachandran, A. Lacis, and G. L. Russell, The GISS global climate/middle atmosphere model, II,

Model variability due to interactions between planetary waves, the mean circulation and gravity wave drag, *J. Atmos. Sci.*, *45*, 371–386, 1988b.

Rind, D., R. Suozzo, N. K. Balachandran, and M. Prather, Climate change and the middle atmosphere, I, The doubled CO_2 climate, *J. Atmos. Sci.*, *47*, 475–494, 1990.

Rind, D., E.-W. Chiou, W. Chu, J. Larsen, S. Oltmans, J. Lerner, M. P. McCormick, and L. McMasters, Overview of the SAGE II water vapor observations: Method, validation and data characteristics, *J. Geophys. Res.*, *98*, 4835–4856, 1993.

Sausen, R., and J. Kohler, Simulating the global transport of nitrogen oxides emissions from aircraft, DLR, Inst. für Phys. der Atmos., *Tech. Rep. 7*, *ISSN 0943-4771*, 1993.

Schumann, U., On the effect of emissions from aircraft engines on the state of the atmosphere, *Ann. Geophys.*, *12*, 365–384, 1994.

Shine, K. P., and A. Sinha, Sensitivity of the Earth's climate to height-dependent changes in the water vapour mixing ratio, *Nature*, *354*, 382–384, 1991.

P. Lonergan and D. Rind, NASA Goddard Space Flight Center, Institute for Space Studies, 2880 Broadway, New York, NY 10025.

(Received August 24, 1994; revised January 7, 1995; accepted January 9, 1995.)